Seismic Response of a Tower as Measured by an Integrated RTK-GPS System

Xiaojing LI, Linlin GE, Gang-Ding PENG, Chris RIZOS, Australia, Yukio TAMURA and Akihito YOSHIDA, Japan

Key words: Structural deformation, digital filtering, GPS, optical fibre sensor, accelerometer

SUMMARY

Monitoring structural response induced by seismic waves is an efficient way to mitigate the damage of earthquakes. For example, the measured signal can be used to activate an alarm system in order to evacuate people from an endangered building, or to drive a control system to suppress earthquake-excited vibrations so as to protect the integrity of the structure, or to assess post-seismic damage to a structure. Traditionally such vibrations have been measured solely by accelerometers. However, it is impossible to measure the static and semi-static components of the movement with accelerometers. An integrated system combining RTK-GPS and accelerometers has been deployed atop a 108m tall tower in Tokyo in order to monitor its structural integrity on a continuous basis. Data acquired during earthquakes are automatically archived.

In this paper, the seismic responses of the tower were analysed using Fast Fourier Transformation (FFT) of the GPS and accelerometer measurements. The data were also converted to displacement (in the case of accelerometer) and acceleration (in the case of GPS) through double-integration and double-differentiation respectively, for the purpose of direct comparison. The results agreed with each other well, except that the static component was missing from the accelerometer-derived results.

In order to determine when a particular signal occurs and fades during a seismic event, a short time FFT analysis was conducted on both the GPS and accelerometer time series. It has been determined that the first order natural frequency of the tower becomes dominant when the seismic waves arrive, and disappears when the event affect is over.

Meanwhile, extensive indoor experiments have been conducted to test optical fibre Bragg grating (FBG) sensors for the measurement of distributed strain. The FBG sensors have demonstrated excellent performance with respect to sensitivity, linearity, repeatability and dynamic range, characteristics which complement the GPS and accelerometer sensors. The FBG system will be installed alongside the GPS and accelerometer sensors when it is ready for field testing.

In this paper the feasibility of integrating advanced sensing technologies such as GPS and FBG with traditional accelerometer sensors, for structural vibration response and deformation monitoring under severe loading conditions, is discussed. The redundancy within the integrated system has shown robust quality assurance for monitoring the health of the tall tower.

Seismic Response of a Tower as Measured by an Integrated RTK-GPS System

Xiaojing LI, Linlin GE, Gang-Ding PENG, Chris RIZOS, Australia, Yukio TAMURA and Akihito YOSHIDA, Japan

1. INTRODUCTION

Civil engineering structures are typically designed based on the principles of material and structural mechanics. Finite element model (FEM) analysis and wind tunnel tests of scaled models are often carried out to assist structural design (e.g., Penman et al, 1999). However, loading conditions in the real world are always much more complicated than can be imagined, and hence key man-made structures must be monitored to ensure that they maintain integrity of design, construction and operation.

In general, until recently, monitoring the dynamic response of civil structures for the purpose of assessment of damage has relied on measurements from accelerometer sensors deployed on the structure. Studies conducted on such data records have been useful in assessing structural design procedures, improving building codes and correlating the response of the structure with the damage caused. However, a double-integration process is required to arrive at the relative displacements, and there is no way to recover the static or quasi-static displacement from the acceleration. Also it is difficult to overcome natural drift of the accelerometer. Therefore, it has been proposed to integrate the accelerometer sensors with GPS and optical fibre sensors in order to best utilise the advantageous properties of each.

In contrast to accelerometers, GPS can measure directly the position coordinates (Parkinson & Spilker, 1996), hence providing an opportunity to monitor, in real-time and full scale, the dynamic characteristics of the structure to which the GPS antennas are attached. In order to achieve cm-level accuracy, the standard mode of precise differential GPS positioning locates one reference receiver at a base station whose three dimensional coordinates are known, so that the second receiver's coordinates are determined relative to this reference receiver.

Preliminary studies have proven the technical feasibility of using GPS to monitor dynamic structural deformation due to winds, traffic, earthquakes and similar loading events in, e.g., the UK (Ashkenazi & Roberts, 1997), USA (Kilpatrick et al, 2003), Singapore (Brownjohn et al, 1998) and Japan (Tamura et al, 2002).

Although GPS offers real-time solutions, it has its own limitations. GPS can only measure the overall deflection of the building and thus little will be revealed regarding the location of the actual displacement causing the deformation. Moreover, GPS can only sample at a rate of up to 20Hz (Trimble, 2003), although higher rates may be soon possible.

On the other hand, optical fibre sensors are increasingly being used in civil engineering structures. Among them the optical Fibre Bragg Grating (FBG) (Kersey et al, 1997) is one of the

most promising new technologies for strain measurement, which can be easily converted to displacement and deformation information. FBG-based sensors have many advantages over conventional electronic sensors. They are characterised by a very good long-term stability and a high reliability, in addition to all the general advantages of glass fibre-based sensors, such as electromagnetic insensitivity, small size, and the possibility to distribute several sensors in one fibre. Embedding the FBG sensors into a structure to obtain useful information both during the construction phase and under extreme loading conditions can be a very efficient means of monitoring the structure's health.

Hence, GPS and FBG are complementary. However, they have rarely been used within a single system. Therefore it has been proposed to integrate them with the traditionally used accelerometer, in order to address the application of structural health monitoring.

The paper is organised as follows. The second part presents an analysis of data collected using GPS and accelerometer sensors while monitoring the responses of a 108m tall steel tower during the earthquake of magnitude Ms 7.0 that occurred on 26 May 2003. The third part introduces the experimental results from a FBG strain measurement system. The fourth part discusses the integration of GPS, FBG and accelerometer sensors. Finally the paper concludes with a summary of the research findings.

2. SEISMIC RESPONSE OF THE TOWER MONITORED BY GPS-ACCELEROMETER

2.1 The Field Experimental System

As part of the collaborative research between the Tokyo Polytechnic University and the University of New South Wales (UNSW), a combined accelerometer and RTK-GPS system has been deployed on a 108m steel tower in Tokyo owned by the Japan Urban Development Corporation, in order to monitor its structural integrity on a continuous basis. At the top of the tower, a GPS antenna together with accelerometers and an anemometer were installed. Another GPS antenna was setup on the top of a 16m high rigid building, as a reference point 110m away from the tower. In addition, strain gauges were set in the base of the tower to measure member stresses. Figure 1 illustrates the experimental setup. Note the local monitoring-coordinate system was established so that X is East, Y is North and Z is pointing to the Zenith. The RTK-GPS and accelerometer data were recorded at 10Hz and 20Hz sampling rates respectively. Data used in this study were collected from 18:00 to 19:00 Japan Standard Time (JST) when an earthquake event of magnitude Ms 7.0 occurred on 26 May 2003 at a depth of 71km.

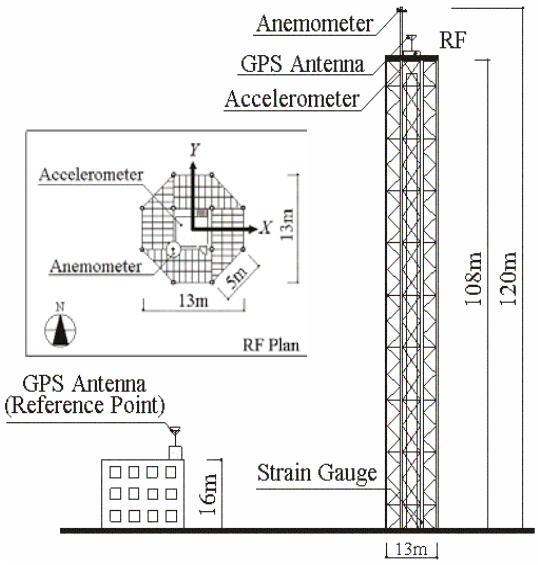

Figure 1: The 108m steel tower for GPS and accelerometer field experiment

2.2 GPS and Accelerometer Data Set

The overall plots of time series of the RTK-GPS measured displacements in X, Y and Z directions are shown in Figure 2. From the least-squares polynomial fitting (blue lines) in Figure 2 the maximum displacements in the X and Y directions are all less than +/-1cm during the two hour period, indicating no significant static or quasi-static movements. But in the Z direction the polynomial fit of the signal seems to suggest vertical ground movement of more than the +/-2cm GPS noise floor and the peak-to-peak fluctuation also averaged over two centimetres after the 1500sec, probably due to surface waves induced by the strong earthquake.

Meanwhile, the S waves caused a peak-to-peak vibration of the tower of more than 6cm in the X and Y directions. However, P waves cannot be seen in the RTK-GPS time series (even when zoomed in). This is because the magnitude of P waves is 2-3 times smaller than the S waves and hence can be buried in the GPS noise. The P waves, however, can be recovered through double-differentiation as demonstrated in Section 2.5.

Measurements from the accelerometers (X and Y directions only) are given in Figure 3. Note the acceleration (Figure 3) has been limited to a period of 300 seconds in order to see both the P and S waves clearly. The peak-to-peak acceleration is almost 200cm/s^2.

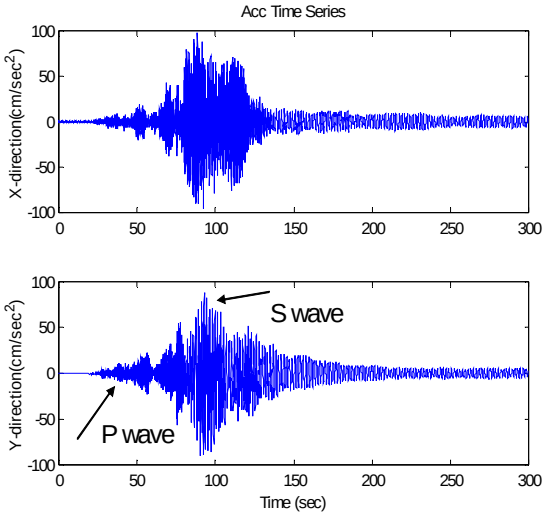

Figure 2: RTK-GPS measured displacements.

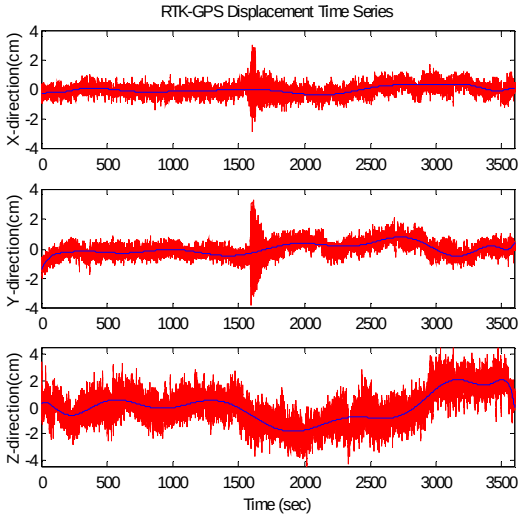

Figure 3: Acceleration time series measured by accelerometers.

2.3 Signals Obtained from Global FFT Analysis

According to a previous study on the basic characteristics and applicability of RTK-GPS (Tamura et al, 2002), GPS results seem to follow closely the actual displacement under conditions when the vibration frequency is lower than 2Hz, and the vibration amplitude is larger than 2cm. Consequently it is possible to assess the accuracy of recorded data by analysing the spectrum of the seismic-induced vibration of the tower. The Fast Fourier Transform (FFT) gives the spectrum of RTK-GPS measurements (Figures 4 and 5). Studying the three spectrums closely, it is obvious that multipath is contributing to all three components, and 0Hz and 0.15Hz are the main frequencies. In the mean time, both X and Y directions show peaks at 0.57Hz and 2.16Hz. There is no clear peak in the Z direction at the expected signals, but signal or noise at the lower frequency end (0-0.8Hz) is much stronger than in the other two directions. This can be partly explained as the static and semi-static movements during the quake affect the tower mostly along the Z direction. This agrees with the time series shown in Figure 2.

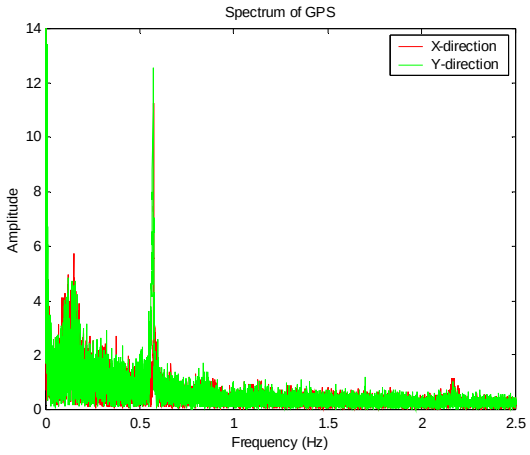

Figure 4: FFT spectrums of GPS for X & Y directions

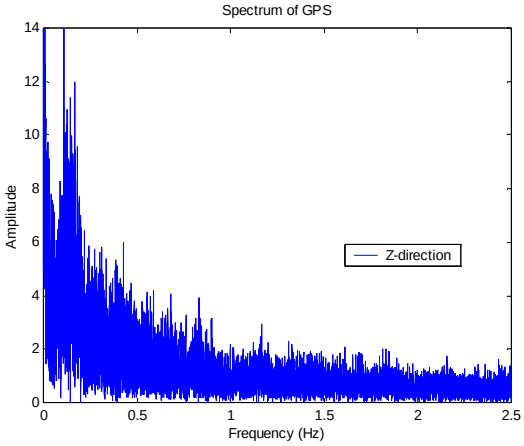

Figure 5: FFT spectrum of GPS for Z direction

The accelerometer's performance during the seismic event is analysed in the same way. Figure 6 is the zoom-in of the FFT spectrum. There are three peaks all in the same locations in the X and Y directions, of which the 0.57Hz and 2.16Hz peaks are identical to the GPS spectrum, while the 4.6Hz as a high order harmonic is not available from the spectrum of GPS.

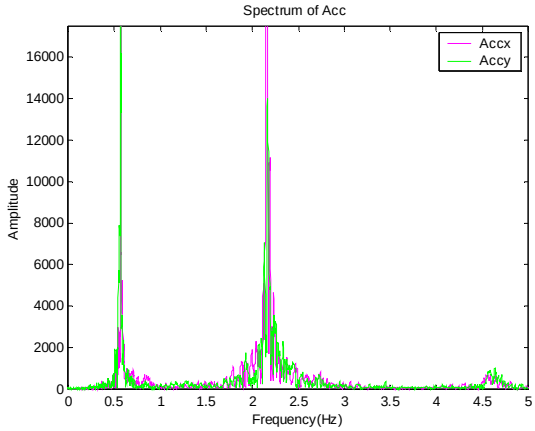

Figure 6: Zoom-in FFT spectrum of the acceleration

It is clear that the spectrums for both the accelerometer and RTK-GPS have the dominant frequency of 0.57Hz, indicating that it is the lowest natural frequency of the steel tower. This result agrees with Tamura et al (2002), using the power spectral density analysis and the RD technique to process the data recorded during a typhoon event. FEM analysis has also confirmed that 0.57Hz is the first mode natural frequency of the tower, 2.16Hz and 4.56Hz are the 2nd mode and 3rd mode respectively (Yoshida et al, 2003). There is no doubt that the GPS and accelerometer are complementary (by comparing Figures 4 and 6).

2.4 Signals Obtained from Short Time FFT Analysis

The results of section 2.3 are obtained by using the usual FFT, whose spectrum represents the frequency composition of the WHOLE time series. It tells the relative strength (amplitude) of the frequency components, but does NOT tell when a particular frequency component occurs or takes over as the most significant frequency. It might be very useful to assess the response of or damage to the structure if it can be detected when a particular frequency component becomes dominant. A way of determining this frequency-time relationship is to apply the FFT to a short segment of the time series each time, or the so-called short time FFT analysis.

Consider the measured digital signal of $x[n]$ as a time series with respect to t. The spectrum $X[f_a]$ obtained by using Fourier transform of a discrete signal (DTFT) is a function of t, which can be derived as follows. First, Fourier transform of a discrete signal (Ambikairajah, 2003) is:

$$X[\theta] = \sum_{n=-\infty}^{\infty} x[n] e^{-jn\theta}, \quad -\pi \le \theta \le \pi \tag{1}$$

Where, $\theta = \omega T$ is the relative frequency, T is sampling period, ω is the frequency in radians.

Considering f_a is the frequency of the signal, then $\omega = 2\pi f_a$. The sampling frequency is determined as $f_s = \frac{1}{T}$. Therefore, θ can be given by:

$$\theta = 2\pi \frac{f_a}{f_s} \tag{2}$$

Then the time length t of the measurements can be calculated by using the sampling period T to multiply the numbers of samples n.

$$t = nT, \quad 0 \le n \le N \tag{3}$$

Substituting Eq. (1) with (2) and (3), Eq. (1) can be rewritten as:

$$X[f_a] = \sum_{n=0}^{N} x[n] e^{-jn2\pi \frac{f_a}{f_s}} = \sum_{n=0}^{N} x[n] e^{-j2\pi f_a nT} = \sum_{n=0}^{N} x[n] e^{-j2\pi f_a t} \tag{4}$$

Hence, from Eq. (4) it can be seen that the frequency f_a of the digital signal $x[n]$ is a function of time t. When t approaches zero, the output frequency from DTFT becomes the instantaneous frequency. In other words, by applying DTFT on small samples of measurements, the frequency-time relationship can be established. The instantaneous frequency output can be expressed as:

$$X[f_a] = \sum_{n=N_1}^{N_2} x[n] e^{-j2\pi f_a t}, \Delta n = N_2 - N_1 \ \& \ t = \Delta nT \tag{5}$$

By taking the samples Δn in power of 2, the efficient algorithm for the short time FFT analysis is obtained.

We can now use Eq. (5) to analyse the tower's frequency response with respect to time during the earthquake event. In order to represent the typical frequency which appeared in the FFT spectrum, it is important to select appropriate number of samples of measurements to be analysed each time, and only the maximum peak is recognised as typical frequency. Figures 7 and 8 are the results from analysing GPS measurements. A total of 256 samples were processed each time. Hence the time length is 25.6s. It can be seen clearly that the tower experienced the strongest vibration lasting for about 7 minutes around 18:30 when the tower's first order natural frequency 0.57Hz became dominant. This cannot be determined from the GPS displacement time series itself because it is too noisy (cf. Figure 2).

It is interesting to see that this duration estimated from accelerometer measurements is about 14 minutes, as shown in Figures 9 and 10. Please note that the starting time for 0.57Hz signal is the same for both GPS and accelerometer. The finishing time is different because the amplitude of seismic waves decreases gradually and when the induced displacement is smaller than the GPS-RTK noise floor it cannot be tracked by GPS anymore. The seismic induced acceleration, however, will continue to be tracked by the accelerometer for as long as 0.57Hz is dominant.

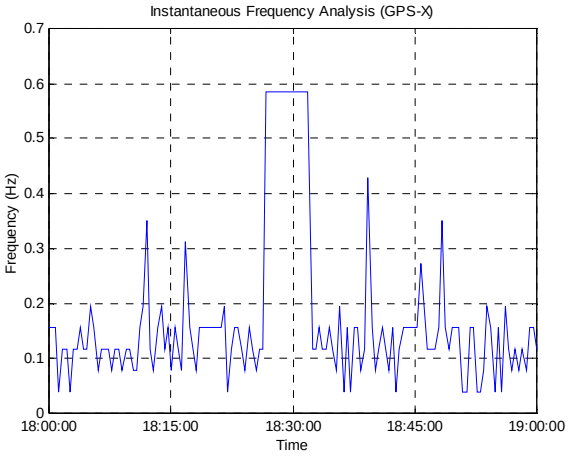

Figure 7: Frequency evolution on GPS x-direction

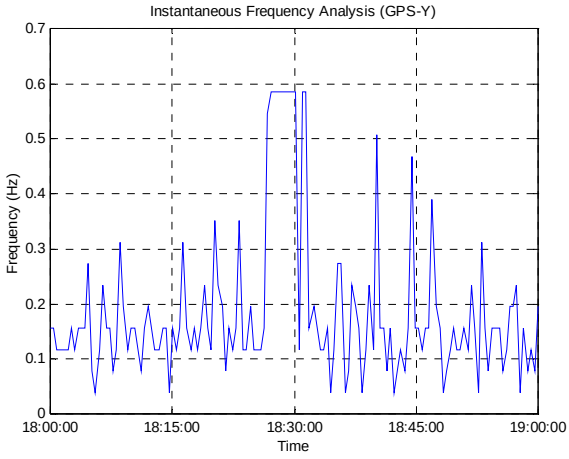

Figure 8: Frequency evolution on GPS y-direction

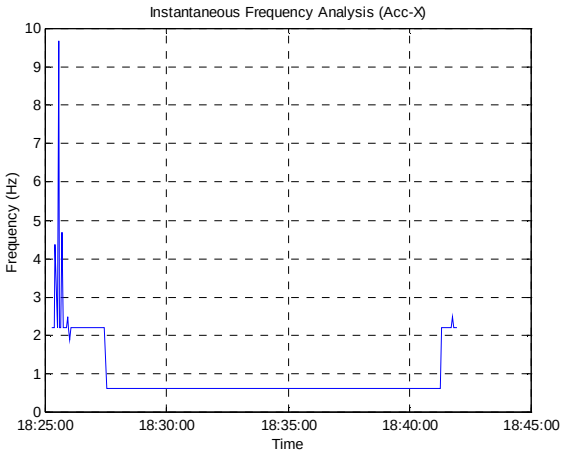

Figure 9: Frequency evolution on Acc x-direction

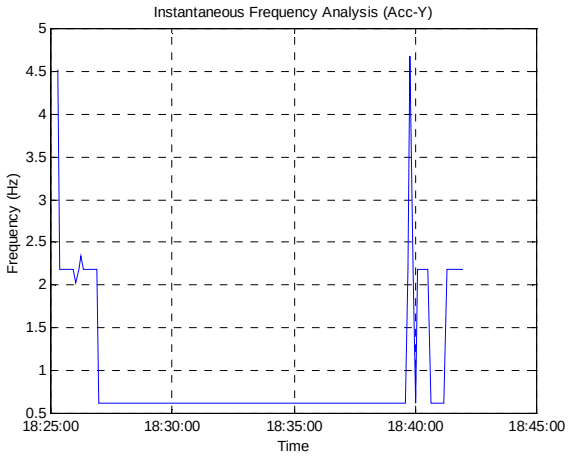

Figure 10: Frequency evolution on Acc y-direction

2.5 Seismic-induced response of the tower: comparison between RTK-GPS and Accelerometer

Response of a structure, especially a tall building, under a severe load generally consists of three components: a static component due to mean force; a quasi-static component caused by the low frequency force fluctuations; and a resonant component caused by the force fluctuation near the structure's first mode natural frequency. Can the integrated GPS and accelerometer system provide all of the required information? The answer is probably "yes". Yet no single sensor can do it alone. From the signal analysis in section 2.3, the GPS sensor gives more information at the low frequency end while the accelerometer sensor gives more at the high frequency end. This means that both of them lose information which is very important for civil engineers. The following analysis will study this problem in more detail.

First, a double-differentiation procedure is applied to a segment of RTK-GPS measured displacement data (both X and Y directions) of 150 seconds duration in order to convert them into acceleration. Figures 11 and 13 show the results of acceleration derived from RTK-GPS measured displacement, compared to accelerometer-measured acceleration. In the figures, the upper plots are the GPS displacement; the middle plots are the acceleration derived from the GPS measurements; and the bottom plots are the accelerometer-measured acceleration. Comparing the time series in the middle and bottom plots, it can be seen that they agree well with each other, although the converted acceleration time series shows high frequency fluctuations due to GPS-specific noise. It is also interesting to see that the P and S seismic waves are clearly visible in the two horizontal directions (X and Y) from the accelerometer data. However, these waves (especially the P waves) are not so obvious from the original GPS displacement time series. After the double-differentiation, the accelerations derived from RTK-GPS also show clearly the seismic waves. Therefore, GPS can be used as a seismometer (Ge, 1999).
In the reverse data processing of Figures 11 and 13, the red and blue in Figures 12 and 14 are displacements directly measured by GPS and derived from accelerometer data through double-

integration respectively. The green and pink lines are the results of their polynomial fitting. From the results shown in Figures 12 and 14, it can be seen that in the dynamic part during the quake the two results agree well with each other. However, significant differences can be seen in the part measured shortly before the quake because the static and quasi-static displacements are also missing from the accelerometer-derived results.

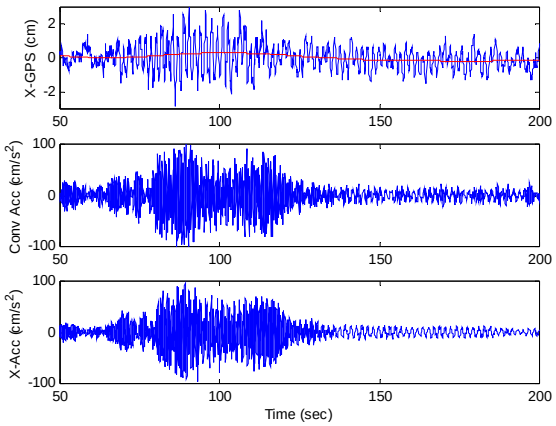

Figure 11: Comparison between RTK-GPS derived and accelerometer-measured accelerations (X-direction**)**

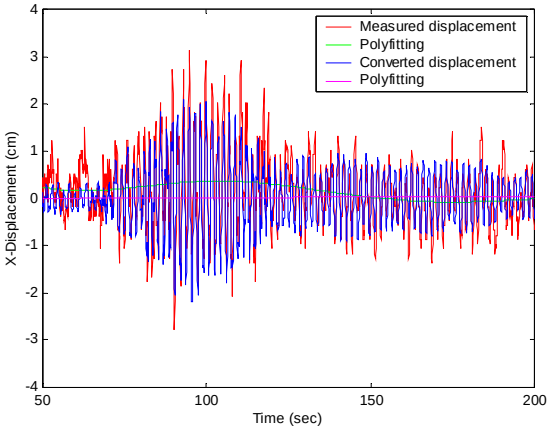

Figure 12: Comparison between RTK-GPS measured and accelerometer-derived displacements (X-direction)

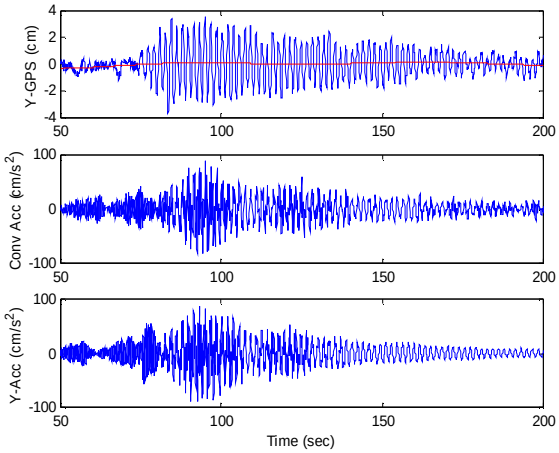

Figure 13: Comparison between RTK-GPS derived and accelerometer-measured accelerations (Y-direction)

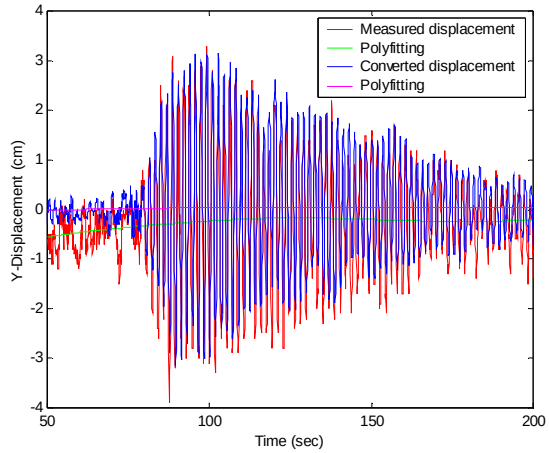

Figure 14: Comparison between RTK-GPS measured and accelerometer-derived displacements (Y-direction)

3. FBG SENSOR FOR STRAIN MONITORING

The Bragg grating in the fibre can be formed by exposing the core of single-mode fibre to an intense optical interference pattern, which effectively creates a single axis strain and temperature sensor on the core of the fibre. The Bragg grating resonance is the central wavelength of light reflected from the Bragg grating, and depends on the effective index of refraction of the fibre core, as well as the periodicity of the grating. Both the effective index of refraction and the periodic pitch between the grating planes will be affected during strain and temperature changes.

Because strain change has been modulated as wavelength shift, and almost all the photo-electrical detectors (PDs) are only sensitive to optical intensity (NOT the wavelength), the straightforward approach of detecting the wavelength shift by using an OSA is a truly expensive option. In order to develop a cost-effective FBG strain monitoring system, it is crucial to design a low-cost, yet sensitive, demodulation scheme so that strain induced wavelength shift can be effectively converted into optical intensity change on the detector. Figure 15 shows a demodulation scheme designed at UNSW.

The system consists of three parts. The first is the strain sensing subsystem consisting of a FBG sensor between A and B in an optic fibre, a broadband source, and a 3 dB coupler. The second part is the tracking subsystem consisting of a FBG filter, piezo-electric transducer (PZT), a 3 dB coupler, two PDs and an oscilloscope. The third part is the control and data acquisition subsystem consisting of a PC, an analog-to-digital converter (ADC), and a stepper motor. The whole system has been developed as a real-time data acquisition, signal processing, and analysing system.

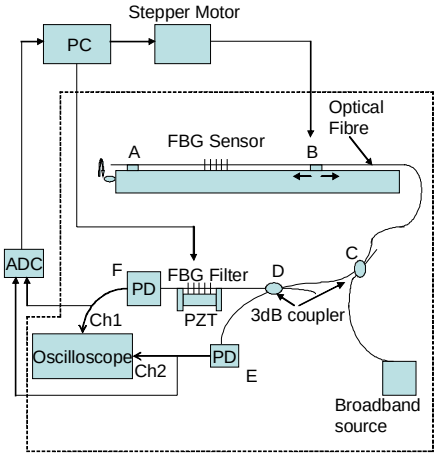

Figure 15: Low-cost FBG strain measurement system

For the optical portion of the system, light generated by the broadband source is injected into the fibre through the coupler C, and then modulated and reflected by the FBG. The reflected light

passes through the coupler C and is split into two parts by the coupler at D: one is directly detected by PD at E, and another passes through FBG filter and detected by PD at F.

For the electrical portion of the system, the PC will control the stepper motor to move fixture B on the slide-track in order to generate strain change on the FBG. The output from PD at E will remain constant because it is NOT sensitive to wavelength shift. On the other hand, the output from PD at F will change with the strain change because wavelength shift introduced at the FBG sensor will damage the alignment between the reflection spectrum of the FBG sensor and the transmission spectrum of the FBG filter (more details later). After the ADC, the PC will be able to pick up this misalignment caused by the strain change on the FBG sensor and then control the PZT to apply the same strain change to achieve a new alignment between the two spectrums. Hence, the strain change at the FBG sensor will be tracked by the PZT.

The measurement is based on strain applied to the sensing FBG, which can be adapted to direct concrete embedding or surface mounting in a real structure, causing the change of output optical intensity through the FBG filter (dotted block of Figure 15). The efficient strain measurement gauge is the length l_{AE} of the fiber. In the system, a pair of 1555nm FBGs has been used, one as the sensor and another as the filter. The oscilloscope receives the voltage signals coming from the photo detectors.

The reflected Bragg wavelength of the sensing FBG is modulated by applied strain, and split into the filter and reference legs. In the filter leg, signal was coupled with the transmitted Bragg wavelength of the filtering FBG and then detected by a photo detector, picked up by Ch1 of the oscilloscope. The reference leg gives the signal intensity level presented in voltage through Ch2. The reflected Bragg spectrum for the sensing FBG is shown in Figure 16, and the central wavelength is 1555.182nm with bandwidth of 0.515nm. Meanwhile, the transmitted Bragg spectrum for the filtering FBG is shown in Figure 17, with the central wavelength at 1555.135nm and bandwidth of 0.405nm.

The initial strain-free condition can give a minimum voltage output from Ch1, because the reflected signal is exactly aligned to the transmitted signal and is attenuated at its maximum. If the two spectrums move away from each other, the output voltage from Ch1 will increase. However, if there is no overlap between them anymore, the output voltage from Ch1 will NOT change even if the strain applied on the sensing FBG continues to increase.

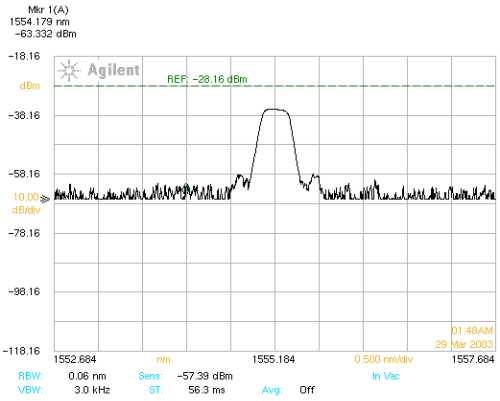

Figure 16: Reflection spectrum of the sensing FBG

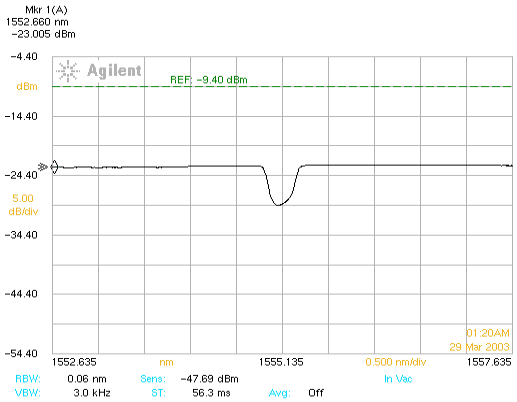

Figure 17: Transmission profile of the filtering FBG

Now set the voltage difference between Ch1 and Ch2 to zero in this stain-free condition, i.e., $\Delta V = V_{Ch1} - C \bullet V_{Ch2} = 0$

C is equivalent to the maximum attenuation of the FBG filter.

Because strain causes the central Bragg wavelength of the sensing FBG to shift, the voltage difference will be no longer zero if the sensing FBG is driven to stretch or release by the stepper motor. The non-zero voltage ΔV will be detected by the PC, and used to control the PZT to stretch or release the filtering FBG in order to induce a compensating wavelength shift. When the two FBGs' Bragg central wavelengths are aligned again, the output voltage becomes zero. The strain deduced from the PZT is precisely the strain applied to the sensing FBG.

The reflected and transmitted Bragg signals have quite different amplitudes due to 95% of the injected light being reflected. Sensing and filtering FBGs have their own slightly different bandwidth although they are paired up. The reflection and transmission Bragg spectrums will have an overlapping range. In order to analyse the accuracy of the system, two types of data were collected. The first one is to read the applied strain with respect to unit output voltage change. Another is to read the output voltage with respect to unit displacement applied. Figures 18 and 19 show the readings. Y1 and Y3 are when the sensing FBG was stretched, and Y2 and Y4 are when it was released gradually. From these results it can be seen that the FBG strain measurement system does have very good performance in terms of sensitivity, linearity, dynamic range, and repeatability.

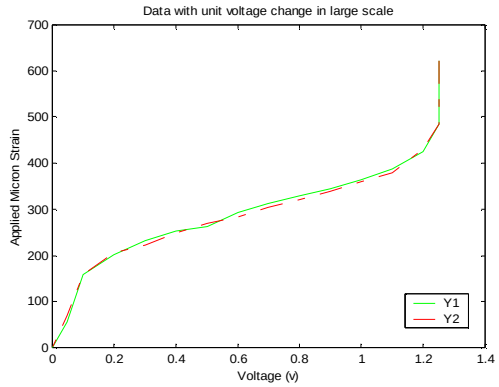

Figure 18: Strain applied on the sensing FBG with respect to unit output voltage change

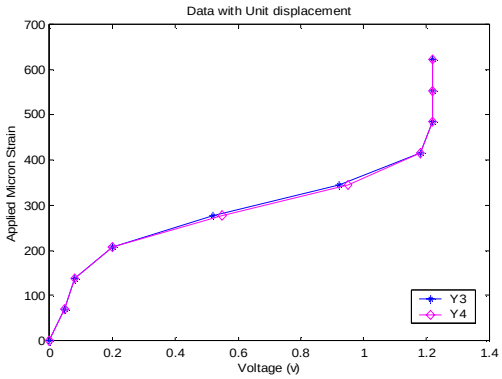

Figure 19: Output voltage with respect to unit displacement applied on the sensing FBG

4. INTEGRATION OF GPS, ACCELEROMETER AND FBG SENSORS

The importance of integrating GPS, accelerometer and FBG sensors for structural health monitoring can be best explained by comparing the overall FFT spectrums of GPS (Figure 20) and accelerometer (Figure 21) measurements during the earthquake. It is possible to zoom in on the figures in the PDF file to read the frequencies corresponding to the peaks. Since the Z direction is not monitored by accelerometer, discussions will focus on X and Y directions.

It can be seen that in general GPS can pick up signals at the low frequency end (0-0.2Hz), probably contaminated by GPS-specific noise such multipath, while it is easier for the accelerometer to record high frequency signals (2Hz and above). *Therefore, the two sensors are complementary.* On the other hand, the two sensors do have some overlapping capability in the band between 0.2 – 2Hz, i.e., whatever is picked up by the accelerometer will also be picked up by the RTK-GPS. *This overlap provides redundancy within the integrated system which enables robust quality assurance* (i.e., double-integration and -differentiation as discussed in section 2) and the overlapping band is likely to increase with the advancement of GPS receiver technology.

From the figures of overall FFT spectrum, it can also be seen that seismic waves are affecting the tower almost equally in the X and Y horizontal directions.

Note currently the RTK-GPS data are collected using the single-base RTK approach. It is possible to enhance the RTK performance by employing network-RTK, especially applicable in Japan considering the available nation-wide, very dense, and continuous GPS (CGPS) network.

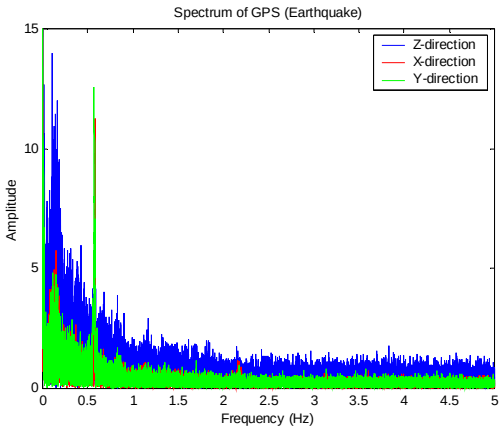

Figure 20: Overall FFT spectrums of GPS measurements during the earthquake

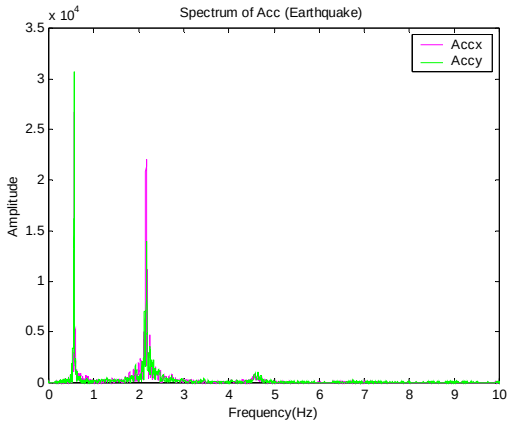

Figure 21: Overall FFT spectrums of accelerometer measurements during the earthquake

In the combined GPS and FBG system, both local strain at the individual FBG sensors and integrated strain between FBG sensors can be monitored. Hence, further redundancy exists in the integrated system. The FBG measured strain can be integrated over the height of the structure and compared to the GPS measured height change of the structure. Or the GPS measured height change can be divided by the height of the structure, giving the average strain which can be compared to the FBG-detected strain.

5. CONCLUSION

GPS and accelerometer sensors have been installed on a 108m tall steel tower and data have been collected at 10Hz and 20Hz during the Ms 7.0 earthquake on 26 May 2003. The earthquake-induced responses of the tower have been analysed in both the time and frequency domains. In the frequency domain, both the GPS and accelerometer results show strong peaks at 0.57Hz, which agrees with previous studies using different methods with typhoon-induced responses, although GPS measurements are noisy in the low frequency end and accelerometer measurements at the high frequency end. Measurements have been converted to displacement (in the case of accelerometer) and acceleration (in the case of GPS) through double-integration and double-differentiation respectively, for the purpose of direct comparison. The results agree with each other very well, except that the static component is missing from the accelerometer-derived results. It has been demonstrated that short time FFT is very effective in determining when signal of a particular frequency becomes dominant.

The results of a series of indoor experiments have shown that the optic fibre Bragg grating (FBG) sensors have demonstrated excellent performance in terms of sensitivity, linearity, repeatability and dynamic range. A low-cost FBG strain measurement system has been developed at UNSW.

The benefits of an integrated system of FBG, GPS and accelerometer sensors to monitor structural deformation have been highlighted.

ACKNOWLEDGEMENTS

The authors, especially the first author, wishes to thanks all members of the Satellite Navigation And Positioning Group (SNAP) and the Photonics and Optical Communications Group (POCG) for useful discussions and help, as well as Mr. Trevor Whitbread for his technical support. Special thanks to Prof Eliathamby Ambikairajah for his encouragement and the Faculty of Engineering of UNSW for the scholarship supporting the 1st author's PhD studies under the joint supervision of the Schools of Surveying and Spatial Information Systems, and Electrical Engineering and Telecommunications. This work would not have been possible without this joint supervision. The research is also sponsored by a Faculty Research Grant of the UNSW.

REFERENCES

Ambikairajah, E., 2003. Digital signal processing lecture notes. School of Electrical Engineering & Telecommunications, the University of New South Wales, Australia.

Ashkenazi, V., & Roberts, G.W., 1997. Experimental monitoring of the Humber Bridge using GPS, *Proc. of Institution of Civil Engineers,* 120, 177-182.

Brownjohn, J., Pan, T.C., Mita, A., & Chow, K.F., 1998. Dynamic and static response of Republic Plaza, *Journal of the Institution of Engineers Singapore,* 38(2) 35-41.

Ge, L., 1999. GPS seismometer and its signal extraction, *Proc. Satellite Division of the Institute of Navigation 12th International Technical Meeting,* September 14-17, Nashville, Tennessee, USA, 41-51.

Kersey, A.D., Davis, M.A., Patrick, H.J. LeBlanc, M., Koo, K.P., Askins, C.G., Putnam, M.A., & Friebele, E.J., 1997. Fiber grating sensors, *Journal of Lightwave Technology,* 15(8), 1442-1463.

Kilpatrick, J., Kijewski, T., Williams, T., Kwon, D.K., Young, B., Abdelrazaq, A., Galsworthy, J., Morrish, D., Isyumov, N., & Kareem, A., 2003. Full scale validation of the predicted response of tall buildings: preliminary results of the Chicago monitoring project, *Proc. 11th Intern. Conf. on Wind Engineering,* June 2-5, Lubbock, Texas, USA.

Parkinson, B., & Spilker, J., 1996. *Global Positioning System: Theory and Applications*, Washington, DC: American Institute of Aeronautics & Astronautics, 793pp.

Penman, A., Saxena, K., & Sharma, V., 1999. *Instrumentation, Monitoring and Surveillance: Embankment Dams,* A.A. Balkema: Rotterdam, 288pp.

Tamura, Y., Matsui, M., Pagnini, L.-C., Ishibashi, R., & Yoshida, A., 2002. Measurement of wind-induced response of buildings using RTK-GPS, *J. Wind Eng. and Industrial Aerodynamics*, 90, 1783-1793.

Tamura, Y., 2003. Design issues for tall buildings from acceleration to damping. *The 11th International Conference on Wind Engineering (11 ICWE),* Lubbock, Texas, USA, June 2-5.

Trimble, 2003. http://www.trimble.com/ms860.html

Yoshida, A., Tamura, Y., Matsui, M., & Ishibashi, S., 2003. Integrity monitoring of builgings by hybrid use of RTK-GPS and FEM analysis, *1st International Conference on Structural Health Monitoring and Intelligent Infrastructure*, November 13-15, Tokyo, Japan.

BIOGRAPHICAL NOTES

Xiaojing Li holds a B.Eng. in Optical Engineering from the Wuhan Technical University of Surveying and Mapping, P.R. China. From 1997 to 1998 she was a research assistant at the Meteorological Research Institute of Japan, researching real-time seismology. She is currently a Ph.D. student at the University of New South Wales (UNSW), Australia, jointly supervised by Professor Chris Rizos of the School of Surveying and Spatial Information Systems and Associate Professor Gang-Ding Peng of the School of Electrical Engineering and Telecommunications. Her research interests are the integration of RTK-GPS, accelerometer, and optical fibre sensors, digital signal processing, and so on.

CONTACTS

Ms Xiaojing Li
School of Electrical Engineering & Telecommunications
School of Surveying and Spatial Information Systems
The University of New South Wales
Sydney, NSW 2052
AUSTRALIA
Tel. + 61 2 9385 4177
Fax + 61 2 9385 5388
Email: xj.li@unsw.edu.au